Journal of Hepatocellular Carcinoma

Dovepress
Taylor & Francis Group

Open Access Full Text Article

ORIGINAL RESEARCH

CECT Radiomics and Liver Fibrosis Markers for Predicting Early Recurrence in Older Patients with Hepatocellular Carcinoma

Fang Liu[1], Zhi Zou[1], Liuchang Zheng[2]

[1]Department of Medical Imaging, Henan Provincial People's Hospital, Zhengzhou, People's Republic of China; [2]Department of Clinical Laboratory, Henan Provincial People's Hospital, Zhengzhou, People's Republic of China

Correspondence: Fang Liu, Email 13676925013@163.com

Purpose: Hepatocellular carcinoma (HCC) carries a high risk of early postoperative recurrence in older patients, and traditional prediction methods are limited by invasiveness and subjectivity. Radiomics studies lack older adult-specific designs and adequate integration of liver fibrosis factors, limiting applicability. Accordingly, we aimed to develop and validate a non-invasive model integrating contrast-enhanced computed tomography (CECT) radiomics and liver fibrosis indicators for predicting early postoperative recurrence in older patients with HCC and identify key risk factors.

Patients and Methods: In total, 169 older patients with HCC (≥60 years) who underwent radical hepatectomy were retrospectively enrolled and randomly assigned to training (n = 131) and validation (n = 38) sets. Radiomics features were derived from preoperative CECT scans acquired during the portal venous phase. The radiomics score (Rad-score) was constructed using the least absolute shrinkage and selection operator algorithm for optimal feature selection. A radiologic–radiomics (RR) nomogram was developed using multivariable logistic regression to identify independent predictors of early recurrence. Model performance was assessed using the area under the curve *AUC), calibration plots, the Hosmer–Lemeshow goodness-of-fit test, and decision curve analysis (DCA).

Results: Sixty-three patients (37.3%) experienced early postoperative recurrence. Tumor diameter, total bilirubin, albumin, type IV collagen, and Rad-score (derived from five optimal radiomics features) were identified as independent predictors. The RR nomogram model achieved AUCs of 0.871 and 0.722 in the training and validation sets, respectively, for predicting early recurrence. Calibration curves and Hosmer–Lemeshow test demonstrated good model calibration ($P > 0.05$); DCA showed a higher net clinical benefit than "treat-all" or "treat-none" strategies across multiple threshold probabilities.

Conclusion: The integrated RR nomogram shows promising discriminatory and calibration ability for predicting early recurrence in older patients with HCC. While this nomogram may serve as a non-invasive preoperative risk-stratification tool, prospective multi-center validation is warranted before clinical adoption.

Keywords: aged, computed tomography, liver fibrosis, liver neoplasms, radiomics

Introduction

Hepatocellular carcinoma (HCC) is the sixth most common tumor globally and the third leading cause of cancer-related deaths, posing a severe threat to human life and health.[1] Hepatic fibrosis is a dysregulated wound-healing response to chronic liver injury, characterized by the accumulation of excessive extracellular matrix, especially collagen. This process, which can progress to cirrhosis, is a major risk factor for HCC. Approximately 90% of HCC cases occur in patients with cirrhosis.[2] With population aging, the proportion of older patients with HCC is increasing. Owing to declining physiological functions and frequent comorbidities, this group faces a higher risk of early postoperative recurrence than younger patients, which affects long-term survival.[3] Early recurrence is a key factor contributing to poor prognosis in older patients with HCC. Therefore, building an accurate early recurrence prediction tool is crucial for optimizing clinical strategies and improving patient outcomes.[3]

https://doi.org/10.2147/JHC.S608338
Received: 10 March 2026
Accepted: 5 May 2026
Published: 19 May 2026

Current clinical methods for evaluating the prognosis and recurrence risk in patients with HCC have limitations. Conventional approaches for predicting HCC recurrence include postoperative pathological assessment of microvascular invasion, serial monitoring of serum alpha-fetoprotein (AFP), and subjective imaging evaluation.[4,5] Although postoperative pathological examination can assess indicators such as tumor grade and microvascular invasion, this procedure is invasive and cannot guide preoperative diagnosis and treatment decisions before surgery. Furthermore, traditional imaging evaluation relies on physicians' subjective judgment of tumor size, shape, and other characteristics, making it difficult to capture the microscopic pathological changes in tumors and liver parenchyma.[6] Serum tumor markers, such as AFP, have limited efficacy in predicting HCC when used alone, with suboptimal sensitivity and specificity.[7] Liver biopsy, the gold standard for evaluation, is associated with potential complications such as bleeding and infection, and older patients have poor tolerance, limiting its clinical application.[8] HCC recurrence is believed to arise from two main mechanisms.[9] The first is the metastasis of the primary tumor within the liver, which typically occurs shortly after surgery and is related to tumor invasiveness. The second is de novo tumor development in the setting of chronic liver disease and fibrosis, which may occur at a later stage. Liver fibrosis creates an inflammatory and fibrotic microenvironment that promotes initial carcinogenesis and subsequent recurrence by altering extracellular matrix composition and impairing immune surveillance.

Contrast-enhanced computed tomography (CECT) is a standard preoperative imaging modality in older patients with HCC. CECT provides clear visualization of liver morphology, tumor location, parenchymal density, and vascular involvement without additional burden, supporting its use in non-invasive prediction.[10] Hepatic fibrosis, a key factor in HCC development, has been linked to tumor recurrence and is reflected by structural changes in the liver on CECT.[11] However, traditional CECT evaluation focuses only on macroscopically visible morphological characteristics and fails to capture quantitative imaging information, resulting in limited predictive performance.[12] Radiomics is an emerging method that employs computational algorithms to extract high-dimensional, quantitative features invisible to the naked eye from medical images.[13,14] It can objectively reflect the microscopic pathological changes in tissues and provide a non-invasive approach for the staging of hepatic fibrosis.[15] Previous studies have demonstrated the potential of CECT-based radiomics models for predicting HCC recurrence. However, most studies have focused on the general adult population, with few studies addressing older patients. Additionally, liver fibrosis-related features are not fully integrated, limiting model applicability and accuracy in older patients.[16]

Accurate prediction of early postoperative recurrence in older patients with HCC remains a clinical requirement, as traditional methods are limited by invasiveness and subjectivity. Existing radiomics studies lack focus on older adults and integration of liver fibrosis, a key prognostic factor, and often show limited generalization owing to single-center designs. In this study, we integrated CECT radiomics with liver fibrosis indicators to develop a non-invasive prediction model for early recurrence in older patients with HCC, identify key markers, and evaluate model performance. Eligible patients were divided into training and validation sets. Radiomics features were extracted to construct a radiomics score (Rad-score), which, combined with clinical and fibrosis data, was used to identify independent risk factors via regression analyses, resulting in a visualized nomogram. Despite the potential of existing radiomics models, few address the unique clinical profile of older patients with HCC or incorporate fibrosis-related biomarkers that may influence recurrence risk. This study addresses a key gap in predicting early recurrence in older patients with HCC by providing a non-invasive and accurate model that outperforms traditional methods and advances radiomics in geriatric liver cancer. It offers a scientific basis for personalized follow-up and intervention strategies to improve prognosis through effective risk stratification.

Materials and Methods

Study Design and Patients

This retrospective study was approved by the Institutional Review Board of Henan Provincial People's Hospital (Approval No. (2022)-(1-233)), and the requirement for informed consent was waived owing to the retrospective design. We confirm that all data used in this retrospective study were anonymized prior to analysis. All identifiers that could link the data to individual participants (including names, medical record numbers, and contact information) were removed. The data were maintained with strict confidentiality and accessed only by the research team for the purposes of this study.

We retrospectively reviewed older patients (aged ≥ 60 years) with HCC who underwent radical hepatectomy at Henan Provincial People's Hospital. Inclusion criteria were as follows:[17] (1) age ≥ 60 years; (2) pathologically confirmed HCC after surgery; (3) CECT within 2 weeks before surgery; (4) complete clinical, laboratory, and imaging data; and (5) patient underwent radical hepatectomy. The exclusion criteria included: (1) a history of previous hepatic surgery, ablation therapy, or preoperative anti-tumor treatments such as transarterial chemoembolization and radiotherapy; (2) coexisting hepatic space-occupying lesions, including hepatic hemangioma and hepatic abscess; (3) poor quality of computed tomography (CT) images; and (4) unqualified liver puncture specimens.

Ultimately, 169 patients were enrolled in this study and randomly assigned to either a training (n = 131) or validation (n = 38) set. The patient selection process is illustrated in Figure 1.

Early postoperative recurrence was defined as HCC recurrence confirmed by imaging or pathology within 6 months after surgery, consistent with the definition of HCC recurrence patterns in the literature.[18] Patients followed institutional protocols and underwent follow-up examinations. After surgery, CECT or magnetic resonance imaging was performed every 3 months.

Collection of Clinical and Laboratory Data

Baseline clinical and laboratory data, including demographics (age and sex) and comorbidities (hypertension and diabetes), were extracted from electronic medical records within 2 weeks before surgery. Tumor-related characteristics, such as tumor diameter and number, were obtained from preoperative imaging reports and confirmed by postoperative pathology.

Fasting venous blood samples were obtained from all patients upon admission, prior to any surgical intervention. Routine laboratory assessments included total bilirubin (TBIL), albumin (ALB), aspartate aminotransferase (AST), alanine aminotransferase, and platelet count. To assess the degree of liver fibrosis, four specific serum fibrosis markers were quantified: hyaluronic acid, procollagen type III N-terminal peptide, type IV collagen (IV-C), and laminin. These markers were detected using radioimmunoassay or enzyme-linked immunosorbent assay kits according to the manufacturers' protocols. Normal reference ranges for all laboratory indicators were established according to our institutional laboratory's standards. All laboratory personnel were blinded to the patients' outcome data during the testing process.

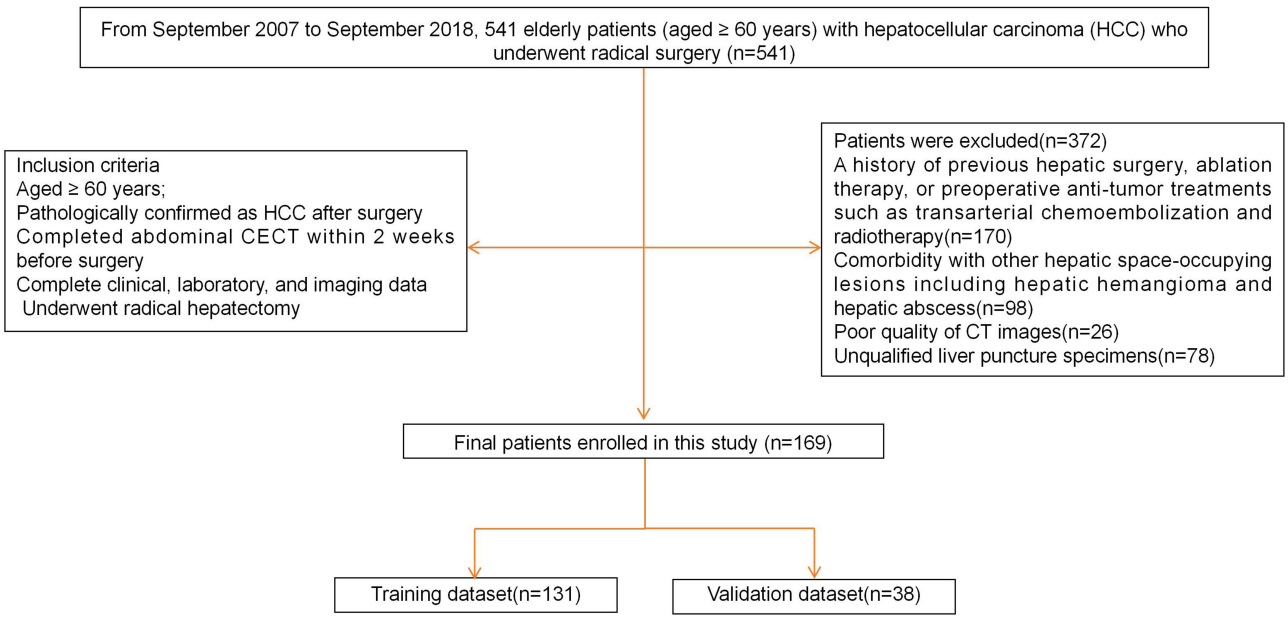

Figure 1 Flow diagram of the study enrolment patients.

https://doi.org/10.2147/JHC.S608338

CT Imaging Protocol

Preoperative CECT examinations were performed using a Siemens Somatom Definition scanner (Siemens Healthineers, Forchheim, Bavaria, Germany) with the following scanning parameters: 120 kVp, 200–250 mA, with 5.0 mm slice thickness and reconstruction interval. Non-ionic iodinated contrast (Iohexol, 300 mg iodine per mL [300 mg I/mL]; GE Healthcare) was injected at a rate of 3.0 mL/s with a weight-based dose of 1.5 mL/kg, consistent with the American College of Radiology guidelines for abdominal CECT.[19,20] Triphasic scans covered the whole liver, including arterial (25–30 s), portal venous (60–70 s), and delayed (180 s) phases.

Image Segmentation and Radiomics Feature Extraction

Region of interest (ROI) segmentation was performed on portal venous phase images by an experienced radiologist using ITK-SNAP software (version 3.8.0; University of Pennsylvania, Philadelphia, PA, USA). The ROI was manually delineated along the tumor margin layer by layer to cover the entire tumor volume, avoiding large vessels and necrotic areas if possible. To assess inter-observer reproducibility, a radiologist independently segmented 30 randomly selected cases. The intra-class correlation coefficient (ICC) was calculated to evaluate feature stability, and features with ICC > 0.80 were considered stable and retained for further analysis.[21]

Radiomics features were extracted using the PyRadiomics package (version 3.0.1; Harvard Medical School, Boston, MA, USA) in Python (version 3.8; Python Software Foundation, Wilmington, DE, USA). Features extracted from each ROI included first-order statistics, shape descriptors, and texture matrices (eg, gray-level co-occurrence matrix [GLCM] and gray-level run length matrix [GLRLM]). Image preprocessing included resampling to a voxel size of $1 \times 1 \times 1$ mm^3 and intensity discretization.

Feature Selection and Radiomics Signature Construction

Feature selection was conducted in the training set to identify the most relevant features associated with early post-operative recurrence. First, the least absolute shrinkage and selection operator (LASSO) regression with 10-fold cross-validation was performed for dimensionality reduction and feature selection (retaining non-zero coefficients). The optimal penalty parameter (λ) was determined based on the minimum binomial deviance criterion. A radiomics signature (Rad-score) was then constructed for each patient using a linear combination of the selected features weighted by their respective LASSO coefficients.

Development and Validation of the Prediction Model

Univariate logistic regression analysis was performed to identify potential risk factors for early recurrence, including clinical characteristics, laboratory indicators, imaging features, and the Rad-score. Variables with $P < 0.05$ in the univariate analysis were entered into multivariable logistic regression to identify independent predictors.

A nomogram was constructed based on the identified independent predictors. Model performance was evaluated via: (1) Discrimination (area under the receiver operating characteristic curve [AUC]); (2) Calibration (calibration curves and Hosmer–Lemeshow test); and (3) Clinical utility (decision curve analysis [DCA]).

Statistical Analysis

The normality of data distribution was assessed using the Shapiro–Wilk test (or Kolmogorov–Smirnov test). Continuous variables were expressed as mean ± standard deviation or median (interquartile range) and compared using the Student's *t*-test or Mann–Whitney *U*-test, as appropriate. Categorical variables were presented as frequencies (percentages) and compared using the Chi-square test or Fisher's exact test. All statistical analyses were performed using R software (version 4.2.1; R Foundation for Statistical Computing, Vienna, Austria) and SPSS (version 26.0; IBM Corp., Armonk, NY, USA). The "glmnet", "rms", "pROC", and "rmda" packages in R were used for LASSO regression, nomogram construction, receiver operating characteristic (ROC) analysis, and DCA, respectively. A two-tailed *P* value < 0.05 was considered statistically significant.

Results

Baseline Characteristics

In the overall cohort, 63 patients (37.3%) experienced early postoperative recurrence, while 106 patients (62.7%) did not. Compared with the non-recurrence group, patients in the recurrence group had significantly larger tumor diameters ($P = 0.008$), higher levels of TBIL ($P = 0.022$), AST ($P = 0.009$), and IV-C ($P = 0.038$), and lower levels of ALB ($P = 0.036$). Additionally, a history of hypertension was more common in the non-recurrence group ($P = 0.049$). These results are presented in Table 1.

As presented in Table 2, a total of 169 older patients with HCC were included in the final analysis, with 131 in the training set and 38 in the validation set. No significant differences were observed in baseline clinical characteristics or laboratory parameters between the training and validation sets ($P > 0.05$ for all), indicating a balanced distribution.

Table 1 Comparison of Baseline Clinical Characteristics Between the Non-Recurrence and Recurrence Groups ($\bar{x} \pm s$, n [%])

Variable	Non-Recurrence Group (n=106)	Recurrent Group (n=63)	t/x^2	*P*
Sex, n (Male, %)	70 (66.04%)	39 (61.90%)	0.295	0.587
Age (years)	75.91±8.02	76.38 ±8.34	0.360	0.720
History of hypertension, n (%)	29 (27.36%)	9 (14.28%)	3.874	0.049
History of Diabetes Mellitus, n (%)	22 (20.75%)	13 (20.63%)	0.000	0.985
History of Coronary Heart Disease, n (%)	12 (11.32%)	8 (12.70%)	0.072	0.789
Tumor diameter, cm (> 5, %)	21 (19.81%)	26 (41.30%)	7.051	0.008
Tumor number (multiple, %)	48 (45.28%)	37 (58.73%)	2.858	0.091
Platelets ($\times 10^9$/L)	157.49±23.48	162.93±26.25	1.393	0.165
TBIL (μmol/L)	19.88±3.83	21.42±4.71	2.315	0.022
ALB (g/L)	36.29±5.75	34.47±4.81	2.111	0.036
AST (U/L)	29.73±3.87	31.41±4.23	2.636	0.009
ALT (U/L)	32.49±5.96	33.71±5.28	1.342	0.181
HA (μg/L)	114.74±13.53	118.43±12.55	1.761	0.080
PIIINP (ng/mL)	11.52±1.77	12.14±1.23	2.44	0.115
IV-C (ng/mL)	67.32±7.64	70.17±9.96	2.089	0.038
LN (ng/mL)	117.52±12.41	122.11±13.98	1.734	0.085

Table 2 Comparison of Clinical and Imaging Factors for Predicting Postoperative Recurrence in the Training and Validation Sets

Variable	Training Dataset			Validation Dataset			*P* (Training vs Validation)
	Non-Recurrence Group (n=82)	Recurrent Group (n=49)	*P*	Non-Recurrence Group (n=24)	Recurrent Group (n=14)	*P*	
Sex, n (Male, %)	28 (34.1%)	23 (46.9%)	0.205	8 (33.3%)	1 (7.1%)	0.151	0.124
Age (years)	74.50 [69.00, 82.00]	75.00 [67.00, 81.00]	0.670	75.00 [69.75, 83.25]	82.00 [72.50, 85.75]	0.203	0.324
History of hypertension, n (%)	23 (28.0%)	8 (16.3%)	0.188	6 (25.0%)	1 (7.1%)	0.349	0.645
History of Diabetes Mellitus, n (%)	16 (19.5%)	8 (16.3%)	0.824	6 (25.0%)	5 (35.7%)	0.740	0.232
History of Coronary Heart Disease, n (%)	8 (9.8%)	5 (10.2%)	1.000	4 (16.7%)	3 (21.4%)	1.000	0.253
Tumor diameter, cm (> 5, %)	14 (17.1%)	19 (38.8%)	0.010	8 (33.3%)	6 (42.9%)	0.811	0.228
Tumor number (multiple, %)	38 (46.3%)	29 (59.2%)	0.214	10 (41.7%)	8 (57.1%)	0.559	0.821
Platelets ($\times 10^9$/L)	157.21 ± 22.58	160.62 ± 25.71	0.428	158.45 ± 26.83	171.00 ± 27.49	0.176	0.316
TBIL (μmol/L)	19.76 ± 3.65	21.46 ± 4.64	0.021	20.30 ± 4.45	21.28 ± 5.12	0.539	0.772
ALB (g/L)	35.89 ± 5.59	34.38 ± 4.93	0.120	37.64 ± 6.21	34.78 ± 4.53	0.141	0.186
AST (U/L)	29.43 ± 3.65	31.02 ± 3.96	0.021	30.77 ± 4.46	32.79 ± 4.97	0.205	0.064
ALT (U/L)	32.07 ± 5.62	33.01 ± 5.12	0.342	33.93 ± 6.93	36.18 ± 5.25	0.301	0.051
HA (μg/L)	113.97 ± 13.16	117.27 ± 12.76	0.162	117.38 ± 14.72	122.49 ± 11.30	0.271	0.061
PIIINP (ng/mL)	11.38 ± 1.66	11.99 ± 1.27	0.028	12.00 ± 2.07	12.66 ± 0.95	0.272	0.059
IV-C (ng/mL)	66.53 [62.26, 71.60]	67.79 [61.97, 74.81]	0.328	68.47 ± 8.53	75.36 ± 8.72	0.023	0.052
LN (ng/mL)	117.66 [108.69, 125.51]	119.88 [109.43, 129.55]	0.223	117.15 ± 13.32	128.60 ± 14.41	0.018	0.248

https://doi.org/10.2147/JHC.S608338

Construction of the Radiomics Signature and Calculation of Rad-Score

Typical CT imaging features of HCC are illustrated in Figure 2. These images highlight key radiological signs used for diagnosis, including the tumor capsule (Figure 2A), smooth tumor margin (Figure 2B), peritumoral enhancement (Figure 2C), as well as intratumoral necrosis and vessels (Figure 2D). These visual characteristics provide the morphological basis for the subsequent extraction of quantitative radiomics features.

To quantify the radiomics information, a Rad-score was constructed for each patient based on the features selected by the LASSO regression algorithm. A total of 22 radiomics features with non-zero coefficients were identified as the optimal subset to predict the risk of postoperative recurrence. These features encompassed various categories, including first-order statistics, texture features (GLCM, gray-level dependence matrix [GLDM], gray-level size zone matrix [GLSZM], and GLRLM), and wavelet-transformed features. The Rad-score was calculated using a linear combination of these 22 features weighted by their respective coefficients. The specific formula is as follows:

Rad-score = (0.0102 * original_firstorder_Kurtosis) + (0.5712 * wavelet.LLH_firstorder_Maximum) + (0.6334 * wavelet.LLH_glcm_ClusterShade) + (0.0766 * wavelet.LHL_firstorder_Mean) + (0.2894 * wavelet.HLL_gldm_SmallDependenceHighGrayLevelEmphasis) + (−0.0789 * wavelet.HLH_firstorder_Mean) + (0.221 * wavelet.HHH_glszm_LargeAreaLowGrayLevelEmphasis) + (0.2193 * wavelet.HHH_gldm_LargeDependenceLowGrayLevelEmphasis) + (1.0121 * log.sigma.2.0.mm.3D_firstorder_Median) + (−0.1297 * log.sigma.2.0.mm.3D_glcm_ClusterShade) + (0.1281 * log.sigma.5.0.mm.3D_glcm_Contrast) + (0.1464 * lbp.3D.m1_glrlm_ShortRunHighGrayLevelEmphasis) + (0.2792 * lbp.3D.m2_glszm_SmallAreaHighGrayLevelEmphasis) + (−0.2425 * diagnostics_Image.interpolated_Minimum.1) + (−0.2066 * original_glcm_ClusterTendency.1) + (0.2605 * wavelet.LLH_firstorder_Skewness.1) + (−0.3287 * wavelet.LHL_firstorder_InterquartileRange.1) + (−0.2803 * wavelet.LHH_firstorder_Skewness.1) + (−0.3249 * wavelet.HLL_gldm_SmallDependenceHighGrayLevelEmphasis.1) + (0.4085 * wavelet.HHH_gldm_DependenceVariance.1) + (0.0439 * log.sigma.3.0.mm.3D_firstorder_Kurtosis.1) + (−0.2867 * log.sigma.3.0.mm.3D_firstorder_Skewness.1). LASSO regression analysis further reduced the dimensionality, identifying five radiomics features with non-zero coefficients as the optimal subset for predicting

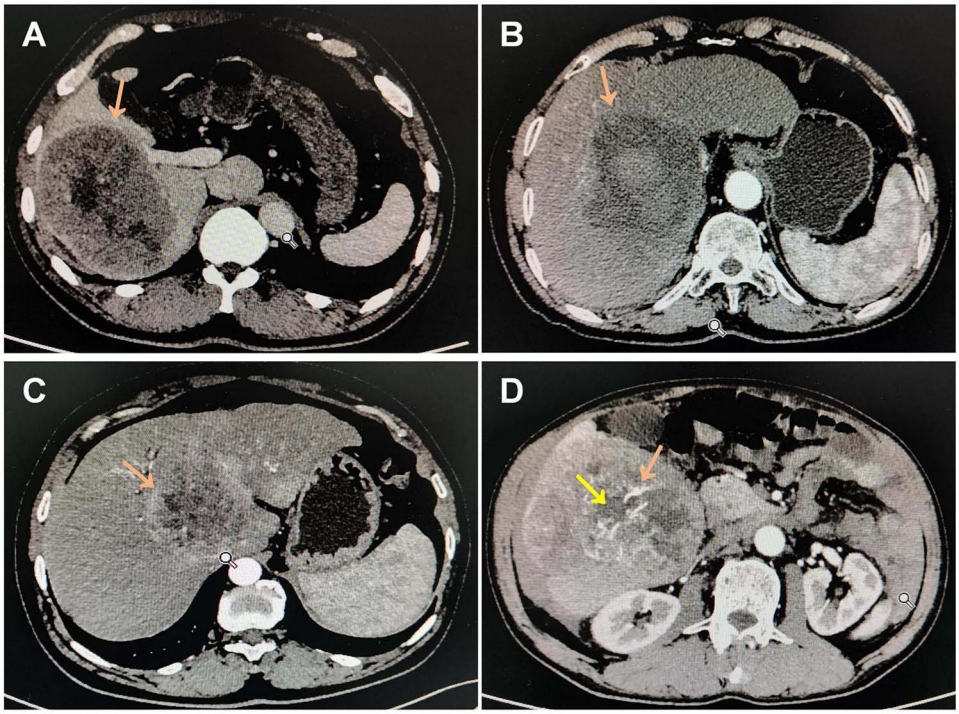

Figure 2 Representative computed tomography (CT) images demonstrating key radiological features of HCC. (**A**) Tumor capsule (Orange arrow): Ring-like high-density appearance surrounding the tumor in the portal venous phase. (**B**) Smooth tumor margin (orange arrow). (**C**) Peritumoral enhancement (orange arrow): Patchy high-density areas outside the tumor range in the arterial phase. (**D**) Intratumoral necrosis (orange arrow): Low-density area in the arterial phase; and intratumoral vessels (yellow arrow): Linear high-density areas in the arterial phase.

https://doi.org/10.2147/JHC.S608338

recurrence, as illustrated in Figure 3A and B. These five features predominantly belong to texture and wavelet-transformed categories, suggesting that spatial heterogeneity and multi-scale intensity patterns, rather than simple shape or first-order statistics, are key imaging correlates of early recurrence in older patients with HCC. This aligns with the hypothesis that aggressive tumors exhibit complex microarchitectural disorganization detectable using radiomics.

Development of the Combined Radiologic–Radiomics (RR) Model

Based on the independent predictors identified through multivariable logistic regression analysis, a combined RR model was constructed to preoperatively predict the risk of postoperative recurrence. The final model incorporated four clinical-

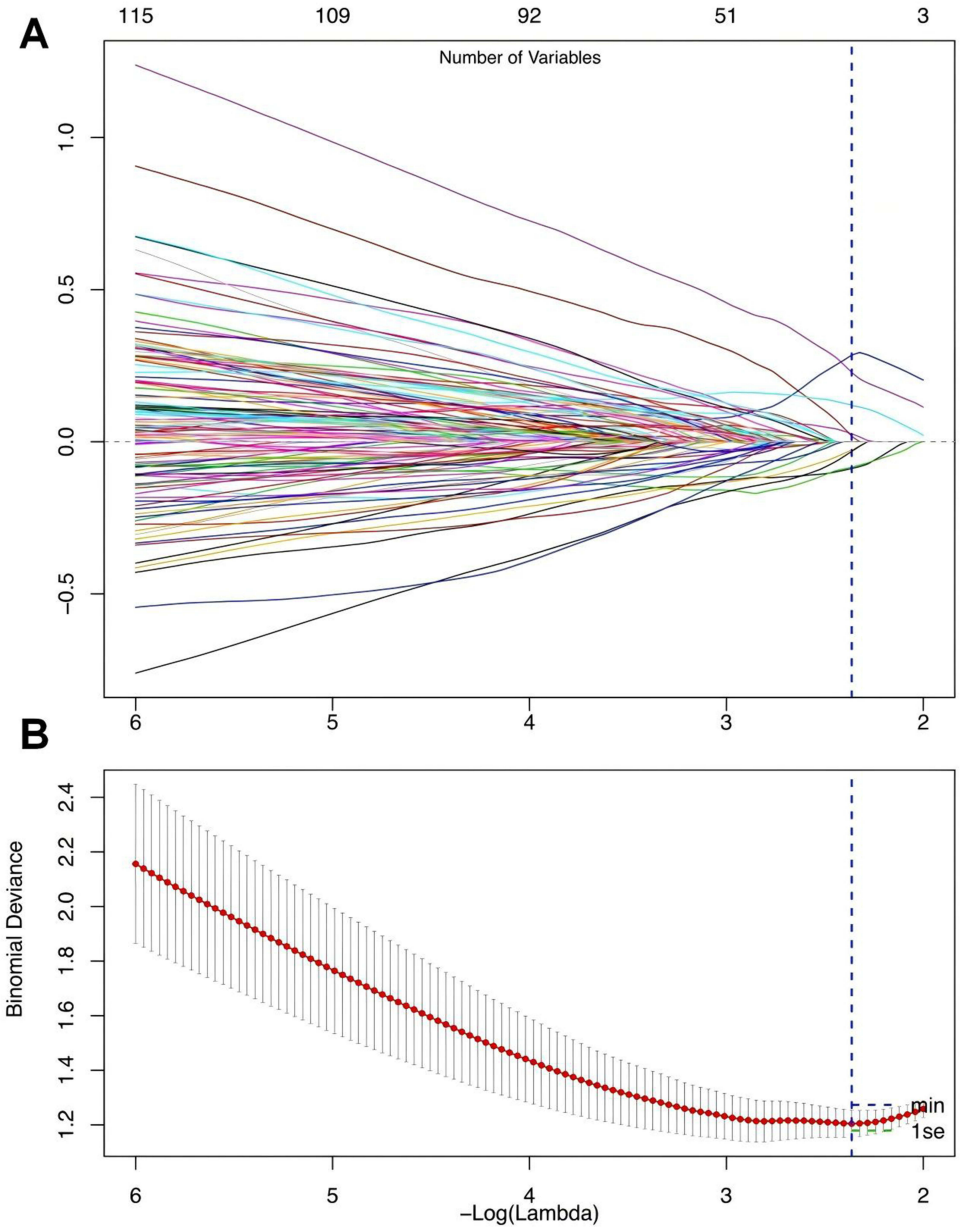

Figure 3 Feature selection using the Least Absolute Shrinkage and Selection Operator (LASSO) regression model. (**A**) LASSO coefficient profiles of the radiomics features. Each colored line represents the coefficient trajectory of one radiomics feature across the LASSO regularization path. The vertical dashed line indicates the optimal λ value selected by 10-fold cross-validation. The five features with non-zero coefficients at this λ (labeled with feature names) constitute the final Rad-score. The vertical dashed line indicates the optimal value of λ selected via 10-fold cross-validation. (**B**) Cross-validation plot for tuning parameter selection in the LASSO model. The binomial deviance is plotted against the log(λ). The left vertical dashed line represents the optimal λ (min criteria), and the right vertical dashed line represents the 1-standard error (1-SE) criteria.

https://doi.org/10.2147/JHC.S608338

Table 3 Multivariate Analysis of Independent Predictors for Postoperative Recurrence in the Training Set

Variables	*P*	Beta	SE	Wald	OR (95% CI)
Tumor diameter, cm (> 5/≤ 5)	0.0210	1.2437	0.8933	1.938	3.47 (1.60–9.98)
TBIL (μmol/L)	0.0280	0.2555	0.1080	5.598	1.29 (1.04–1.60)
ALB (g/L)	0.0350	−0.2702	0.0925	8.525	0.76 (0.64–0.92)
IV-C (ng/mL)	0.0090	0.1371	0.0579	5.612	1.15 (1.02–1.28)
Wavelet.HLL_gldm_SmallDependenceHighGrayLevelEmphasis	0.0040	0.0040	0.0017	5.280	1.00 (1.00–1.01)
Wavelet.HLH_firstorder_Mean	0.0260	−0.4711	0.2179	4.675	0.62 (0.41–0.96)
Wavelet.HHH_gldm_LargeDependenceLowGrayLevelEmphasis	0.0390	0.2986	0.1602	3.473	1.35 (0.98–1.85)
Log.sigma.2.0.mm.3D_firstorder_Median	< 0.001	0.1409	0.0426	10.956	1.15 (1.06–1.25)
Log.sigma.2.0.mm.3D_glcm_ClusterShade	0.0050	−0.0018	0.0009	4.227	1.00 (1.00–1.00)

radiological factors (tumor diameter, TBIL, ALB, and IV-C) and the calculated Rad-score. The predictive logit function and the individual probability of recurrence were expressed as follows:

Y = β0 + 1.2437 × Tumor diameter + 0.2555 × TBIL − 0.2702 × ALB + 0.1371 × IV-C + 1.0 × Rad-score (Variable Definitions and Legend: β0: The constant term of the regression model. X_1: wavelet.HLL_gldm_SmallDependence HighGrayLevelEmphasis; X_2: wavelet.HLH_firstorder_Mean; X_3: wavelet.HHH_gldm_LargeDependence LowGrayLevel Emphasis; X_4: log.sigma.2.0.mm.3D_firstorder_Median; X_5: log.sigma.2.0.mm.3D_glcm_Cluster Shade; Tumor diameter: Assigned as 1 for > 5 cm and 0 for ≤ 5 cm.; TBIL, ALB, IV-C: represent the raw values obtained from laboratory examinations).

In the multivariable logistic regression analysis of the training set, tumor diameter (>5 cm vs ≤5 cm) (odds ratio [OR] = 3.47, 95% confidence interval [CI]: 1.60−9.98, $P = 0.021$), TBIL (OR = 1.29, 95% CI: 1.04−1.60, $P = 0.028$), ALB (OR = 0.76, 95% CI: 0.64−0.92, $P = 0.035$), IV-C (OR = 1.15, 95% CI: 1.02−1.28, $P = 0.009$), and the Rad-score (derived from five radiomics features), were identified as independent predictors of early postoperative recurrences (Table 3). Based on the RR model, a nomogram was generated to visually estimate recurrence probability (Figure 4). Each predictor contributes a specific number of points, and the sum of these points corresponds to the predicted risk of recurrence.

Performance and Validation of the RR Model

The discriminatory ability of the RR model was evaluated using ROC curve analysis. In the training set, the combined model achieved an AUC of 0.871 (95% CI: 0.79–0.93), demonstrating superior performance compared to any single clinical indicator or the radiomics signature alone. In the validation set, the model maintained robust predictive accuracy, with an AUC of 0.722 (95% CI: 0.61–0.87) (Figure 5).

Furthermore, calibration curves demonstrated good agreement between predicted probabilities and observed recurrence rates in both the training and validation sets (Figure 6A and B). Calibration was assessed using the Hosmer–Lemeshow test, where P > 0.05 suggests no significant deviation between predicted and observed recurrence rates across risk deciles. Furthermore, DCA showed that the RR model provided a higher net benefit than the "treat-all" or "treat-none" strategies across a wide range of threshold probabilities, confirming its potential clinical utility for guiding postoperative management decisions (Figure 6C).

Discussion

HCC is a major global health concern and ranks as the third leading cause of cancer-related deaths worldwide.[22] The increasing incidence of HCC, particularly among older patients, poses unique clinical challenges owing to the complexity of their comorbidities and the need for tailored treatment strategies.[23] Older patients often present with distinct tumor biology and may respond differently to therapies compared with younger populations.[24,25] Accordingly, understanding the risk factors associated with early recurrence in this demographic is crucial for optimizing postoperative management and improving outcomes.

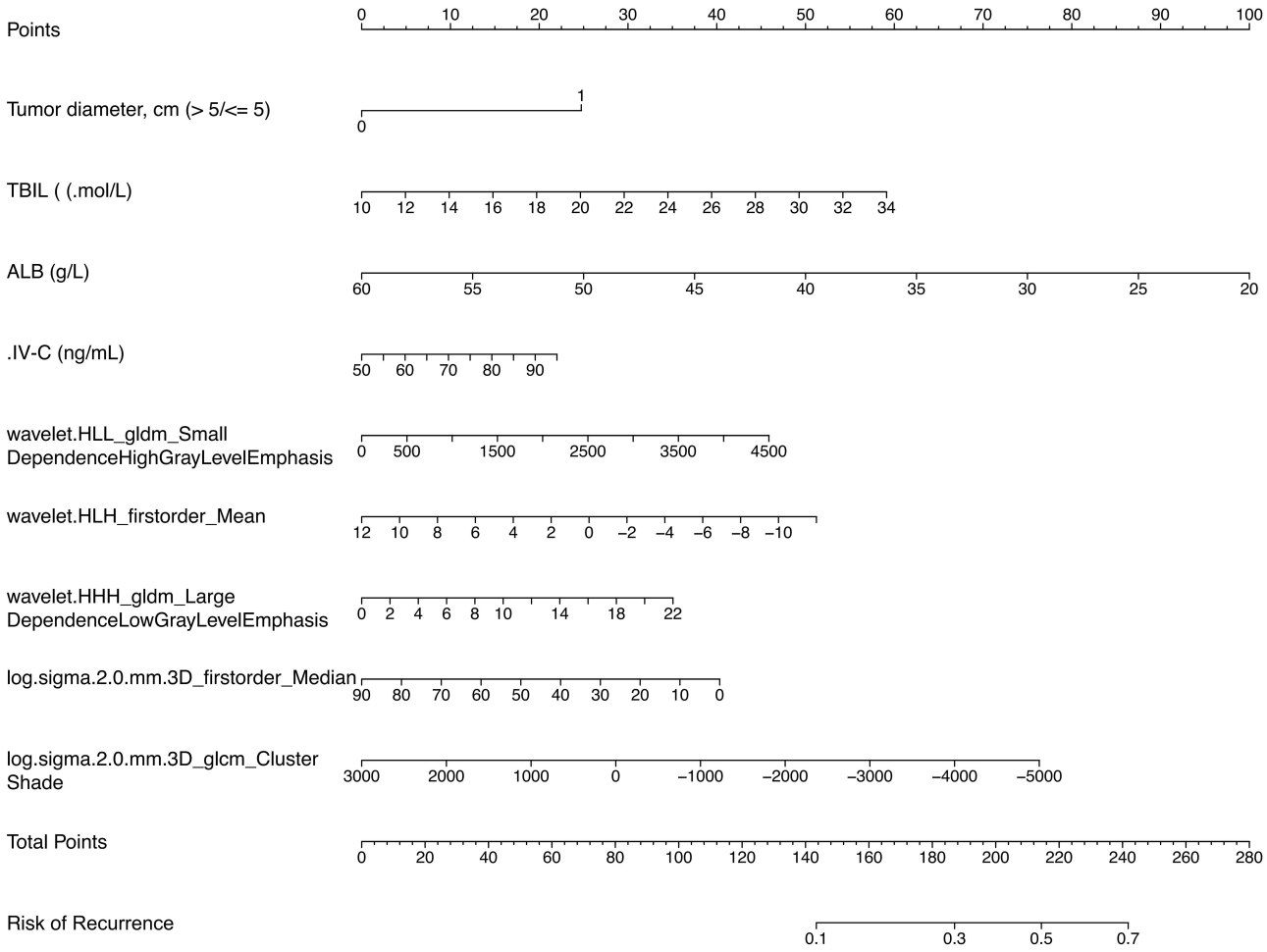

Figure 4 The established radiomics nomogram for predicting postoperative recurrence of HCC.

In this study, we explored early postoperative recurrence in older patients with HCC, focusing on integrating quantitative radiomics data from preoperative imaging with clinical and laboratory variables to enhance risk stratification. Our findings revealed that a radiomics signature, in conjunction with factors such as tumor diameter and serum biomarkers, could effectively predict early recurrence rates. The development of a combined RR model demonstrated notable predictive performance, indicating its potential utility in clinical practice for guiding individualized treatment and postoperative surveillance in this vulnerable patient population.[26–29] In older patients with HCC, early recurrence poses a therapeutic dilemma: aggressive interventions may compromise quality of life, while passive surveillance risks missing the window for curative salvage. Our RR nomogram addresses this issue by providing a preoperative, non-invasive risk estimate that may guide shared decision-making, for example, identifying candidates for intensified adjuvant therapy or closer imaging follow-up. Unlike models based solely on tumor morphology, our integration of fibrosis biomarkers reflects the dual importance of tumor biology and liver parenchymal status in recurrence pathogenesis.

We observed that factors such as tumor diameter, TBIL, ALB, and IV-C play crucial roles in predicting early recurrence in older patients with HCC. The association between larger tumor diameter and early recurrence observed in our cohort aligns with the hypothesis that bigger tumors are more likely to harbor microscopic vascular invasion or satellite nodules, which may seed early intrahepatic recurrence despite macroscopically complete resection. This underscores the value of incorporating size into risk prediction models. The multivariable logistic regression analysis identified tumor diameter >5 cm and elevated TBIL as independent predictors of early recurrence, with ORs indicating a clear association between these variables and patient outcomes.[30] Elevated TBIL may reflect impaired liver function, which could contribute to tumor progression and

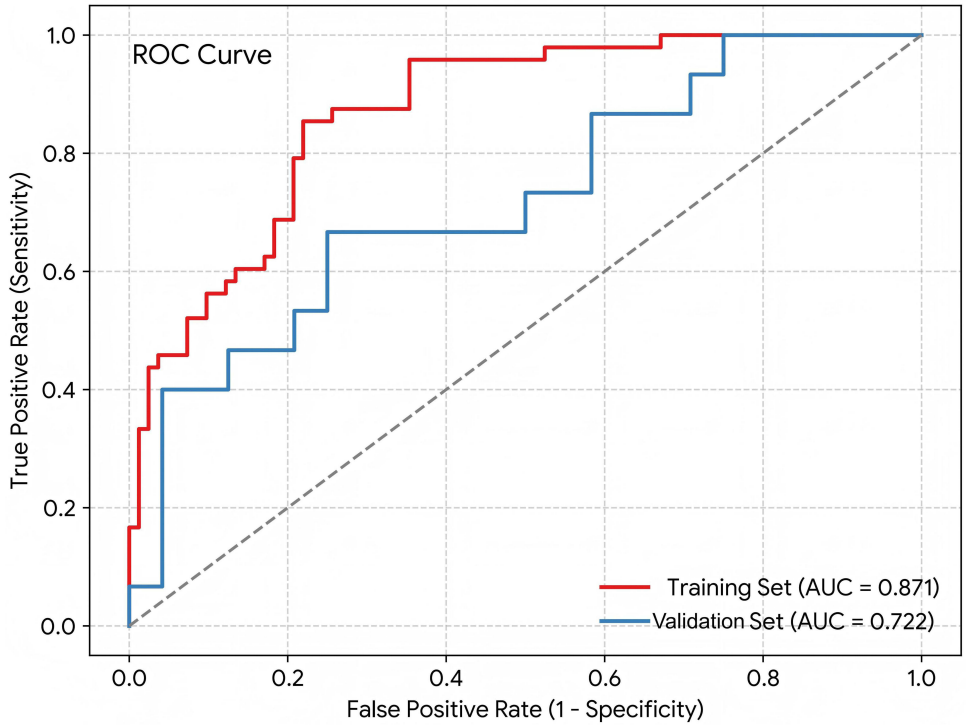

Figure 5 Receiver operating characteristic (ROC) curves of the radiomics signature in the training and validation sets.

recurrence after surgery.[31] Furthermore, low ALB levels suggest poor nutritional status and liver reserve, both of which are critical determinants of postoperative recovery and recurrence risk.[32]

The integration of these clinical variables into an RR nomogram model yielded promising results for identifying high-risk patients. The model demonstrated an AUC of 0.871 in the training set and 0.722 in the validation cohort, indicating robust predictive performance. The clinical utility of this model lies in its ability to guide tailored postoperative surveillance strategies, particularly for older patients who often exhibit different disease characteristics and treatment responses compared with younger cohorts.[33] Regarding practical relevance, the model enables clinicians to identify high-risk older patients preoperatively, potentially guiding decisions on adjuvant therapy intensity or surveillance frequency, as highlighted in recent studies.[34–36]

Our findings are consistent with existing literature, which emphasizes the need for personalized risk stratification tools in managing older patients with HCC. Previous studies have reported similar associations between elevated TBIL and recurrence rates in varying populations, reinforcing the notion that liver function and tumor biology are intricately linked in influencing patient outcomes.[37] In summary, our study underscores the importance of considering both clinical and radiomics features for effective preoperative risk stratification in older patients with HCC, potentially leading to improved management strategies in this vulnerable population.

The limitations of this study primarily stem from its retrospective and single-center design, which may introduce selection bias and limit the generalizability of the findings. The moderate sample size, particularly the validation set of only 38 patients, raises concerns regarding statistical power and increases the risk of overfitting in model development. Furthermore, while the internal validation demonstrated promising results, the lack of external validation in independent datasets limits the assessment of model robustness across diverse clinical settings. Manual segmentation of imaging data, although assessed for inter-observer reproducibility, introduces variability that affects clinical applicability. Additionally, the study did not explore the biological validation of the radiomics features, leaving potential connections between imaging characteristics and underlying tumor biology unexamined. Finally, information on postoperative adjuvant therapies was not systematically collected, and such treatments may have influenced recurrence patterns. Future prospective studies should account for this confounding factor.

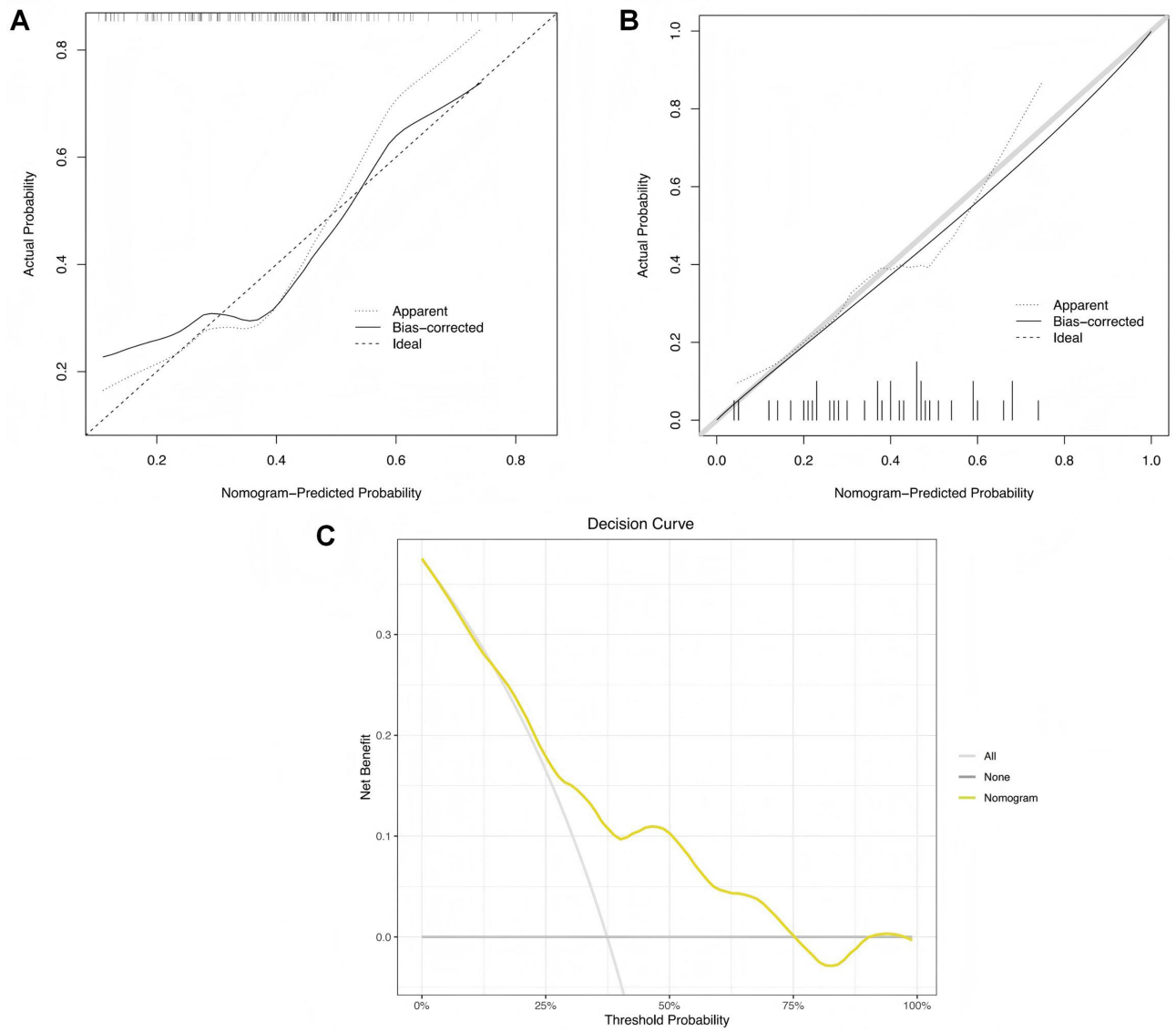

Figure 6 Calibration curves and Decision Curve Analysis (DCA) of the nomogram. (**A** and **B**) Calibration curves for the nomogram in the training set (**A**) and validation set (**B**). The x-axis represents the nomogram-predicted probability of recurrence, and the y-axis represents the actual observed frequency. The dotted gray line represents the apparent performance, the solid black line represents the bias-corrected performance (via bootstrapping), and the dashed diagonal line represents the ideal reference. (**C**) Decision curve analysis for the nomogram. The x-axis indicates the threshold probability, and the y-axis measures the net benefit. The yellow line represents the nomogram, the gray line represents the assumption that all patients will recur ("All"), and the horizontal black line represents the assumption that no patients will recur ("None").

Conclusion

In conclusion, this study presents a novel integrated RR nomogram for predicting early postoperative recurrence in older patients with HCC, demonstrating substantial discriminatory ability and calibration. The identification of key clinical and radiomics predictors offers a practical tool for preoperative risk stratification, potentially enhancing personalized post-operative surveillance and treatment strategies. Despite limitations, including the need for prospective validation and further exploration of the biological relevance of radiomics features, the findings underscore the potential utility of this model in optimizing patient management and outcomes in a growing population of older patients with HCC.

Data Sharing Statement

All the results are presented in the article. Further inquiries can be directed to the corresponding authors.

https://doi.org/10.2147/JHC.S608338

Ethics Statement

This study was approved by the Institutional Review Board of Henan Provincial People's Hospital (Approval No. (2022) - (1-233)), which waived the requirement for informed consent due to the retrospective nature of the research. All experiments and procedures were performed according to the Declaration of Helsinki (as revised in 2013). We confirm that all data used in this retrospective study (Prediction of early postoperative recurrence in elderly patients with hepatocellular carcinoma based on contrast-enhanced computed tomography and liver fibrosis characteristics) were anonymized prior to analysis. All identifiers that could link the data to individual participants (including names, medical record numbers, and contact information) were removed. The data were maintained with strict confidentiality and accessed only by the research team for the purposes of this study.

Author Contributions

All authors made a significant contribution to the work reported, whether that is in the conception, study design, execution, acquisition of data, analysis and interpretation, or in all these areas; took part in drafting, revising or critically reviewing the article; gave final approval of the version to be published; have agreed on the journal to which the article has been submitted; and agree to be accountable for all aspects of the work.

Funding

There is no funding to report.

Disclosure

The authors report no conflicts of interest in this work.

References

1. Pol S. Hepatocellular carcinoma (HCC). *Med Trop Sante Int*. 2024;4(4):. doi:10.48327/mtsi.v4i4.2024.614 Serbian
2. Liu Y, Cong K, Li Q, Zhang D, Sheng J. New insights into combined immunotherapy for hepatocellular carcinoma associated with liver cirrhosis. *Front Immunol*. 2025;16:1741398. doi:10.3389/fimmu.2025.1741398
3. Tang X, Wang Q, Jin R, Hu C. A novel nomogram to predict prognosis in elderly early-stage hepatocellular carcinoma patients after ablation therapy. *J Hepatocell Carcinoma*. 2024;11:901–911. doi:10.2147/jhc.S459250
4. Yamamoto K, Imamura H, Matsuyama Y, et al. AFP, AFP-L3, DCP, and GP73 as markers for monitoring treatment response and recurrence and as surrogate markers of clinicopathological variables of HCC. *J Gastroenterol*. 2010;45(12):1272–1282. doi:10.1007/s00535-010-0278-5
5. Yang C, Liang Z, Zhao L, Li R, Ma P. Prediction of microvascular invasion in hepatocellular carcinoma using a preoperative serum C-reactive protein-based nomogram. *Sci Rep*. 2025;15(1):522. doi:10.1038/s41598-024-84835-w
6. Wang L, Xu HX, Wang R, et al. Advances in multi-omics studies of microvascular invasion in hepatocellular carcinoma. *Eur J Med Res*. 2025;30 (1):165. doi:10.1186/s40001-025-02421-w
7. Suner A, Carr BI, Akkiz H, et al. C-reactive protein and platelet-lymphocyte ratio as potential tumor markers in low-alpha-fetoprotein hepatocellular carcinoma. *Oncology*. 2019;96(1):25–32. doi:10.1159/000492473
8. Zhou F, Stueck A, McLeod M. Liver biopsy complication rates in patients with non-alcoholic fatty liver disease. *Can Liver J*. 2022;5(2):106–112. doi:10.3138/canlivj-2021-0019.
9. Gu J, Liang BY, Zhang EL, Zhang ZY, Chen XP, Huang ZY. Scientific hepatectomy for hepatocellular carcinoma. *Curr Med Sci*. 2023;43 (5):897–907. doi:10.1007/s11596-023-2761-2
10. Kan NN, Yu CY, Cheng YF, et al. Combined Hounsfield units of hepatocellular carcinoma on computed tomography and PET as a noninvasive predictor of early recurrence after living donor liver transplantation: time-to-recurrence survival analysis. *Eur J Radiol*. 2024;177:111551. doi:10.1016/j.ejrad.2024.111551
11. Tietz E, Truhn D, Müller-Franzes G, et al. A radiomics approach to predict the emergence of new hepatocellular carcinoma in computed tomography for high-risk patients with liver cirrhosis. *Diagnostics*. 2021;11(9). doi:10.3390/diagnostics11091650
12. He HB, Jin XC, Liu YC, et al. Clinical value of contrast-enhanced ultrasound combined with quantitative analysis in Bosniak ≥ II cystic renal masses. *Abdom Radiol*. 2025;50(7):3069–3083. doi:10.1007/s00261-024-04744-4
13. Aerts HJ, Velazquez ER, Leijenaar RT, et al. Decoding tumour phenotype by noninvasive imaging using a quantitative radiomics approach. *Nat Commun*. 2014;5(1):4006. doi:10.1038/ncomms5006
14. van Timmeren JE, Cester D, Tanadini-Lang S, Alkadhi H, Baessler B. Radiomics in medical imaging-"how-to" guide and critical reflection. *Insights Imaging*. 2020;11(1):91. doi:10.1186/s13244-020-00887-2
15. Kanki A, Maeba K, Sotozono H, et al. Evaluation of liver fibrosis using hepatic extracellular volume fraction by contrast-enhanced computed tomography before and after direct-acting antiviral therapy in patients with chronic hepatitis C infection: comparison with serological liver fibrosis markers. *Br J Radiol*. 2021;94(1127):20210045. doi:10.1259/bjr.20210045
16. Li J, Chen Z, Wang Q, Du X, Zhang J. Radiomics model based on preoperative contrast-enhanced CT and clinical features for predicting early recurrence of hepatocellular carcinoma. *Ann Ital Chir*. 2025;96(6):771–782. doi:10.62713/aic.3902
17. Deng H, Tong XQ, Jiang ZA, et al. Practical application of ERAS protocols in older adults with hepatocellular carcinoma undergoing hepatectomy: a propensity score matching study. *Clin Interv Aging*. 2026;21:544770. doi:10.2147/cia.S544770

18. Tanemura A, Noguchi D, Shinkai T, et al. Prognostic significance of early and multiple recurrences after curative resection for hepatocellular carcinoma. *BMC Surg*. 2024;24(1):339. doi:10.1186/s12893-024-02642-6
19. Du Y, Wang YN, Wang Q, et al. A comparison of the use of contrast media with different iodine concentrations for enhanced computed tomography. *Front Physiol*. 2023;14:1141135. doi:10.3389/fphys.2023.1141135
20. George AJ, Manghat NE, Hamilton MC. Comparison between a fixed-dose contrast protocol and a weight-based contrast dosing protocol in abdominal CT. *Clin Radiol*. 2016;71(12):1314.e1–1314.e9. doi:10.1016/j.crad.2016.07.009
21. Zwanenburg A, Vallières M, Abdalah MA, et al. The image biomarker standardization initiative: standardized quantitative radiomics for high-throughput image-based phenotyping. *Radiology*. 2020;295(2):328–338. doi:10.1148/radiol.2020191145
22. Taniguchi H. Liver Cancer 2.0. *Int J Mol Sci*. 2023;24(24):17275. doi:10.3390/ijms242417275
23. Bardhi O, Daher D, Patel M, et al. Impact of age on clinical outcomes among patients with hepatocellular carcinoma: a systematic review and meta-analysis. *JHEP Rep*. 2025;7(6):101368. doi:10.1016/j.jhepr.2025.101368
24. Lyu N, Yi JZ, Zhao M. Immunotherapy in older patients with hepatocellular carcinoma. *Eur J Cancer*. 2022;162:76–98. doi:10.1016/j.ejca.2021.11.024
25. Zhang D, Zhu Y, Shen Z, Ma S, Liu S, Lu Z. Immunosenescence and immunotherapy in elderly patients with hepatocellular carcinoma. *Semin Cancer Biol*. 2025;111:60–75. doi:10.1016/j.semcancer.2025.02.010
26. Harada M, Aramaki O, Midorikawa Y, et al. Impact of patient age on outcome after resection for hepatocellular carcinoma. *Biosci Trends*. 2021;15(1):33–40. doi:10.5582/bst.2020.03437
27. Shehta A, Medhat M, Farouk A, et al. Liver resection for hepatocellular carcinoma in elderly patients: does age matter? *BMC Surg*. 2024;24(1):248. doi:10.1186/s12893-024-02528-7
28. Liu YW, Yong CC, Lin CC, et al. Liver resection in elderly patients with hepatocellular carcinoma: age does matter. *Updates Surg*. 2021;73(4):1371–1380. doi:10.1007/s13304-021-01021-7
29. Lee HA, Lee S, Lee HL, et al. The efficacy of treatment for hepatocellular carcinoma in elderly patients. *J Liver Cancer*. 2023;23(2):362–376. doi:10.17998/jlc.2023.08.03
30. Li Y, Zu X, Hu X, Zhao C, Mo M, Fan B. Competing endogenous RNA network analysis reveals pivotal ceRNAs in bladder urothelial carcinoma. *Transl Androl Urol*. 2021;10(2):797–808. doi:10.21037/tau-20-1167
31. Zhao M, Feng J, Tang L. Competing endogenous RNAs in lung cancer. *Cancer Biol Med*. 2021;18(1):1–20. doi:10.20892/j.issn.2095-3941.2020.0203
32. Dini V, Michelucci A, Granieri G, Zerbinati N, Margiotta FM, Romanelli M. Evaluation of post-surgical complications of hidradenitis suppurativa lesions explored with presurgical ultra-high frequency ultrasound mapping. *J Wound Care*. 2024;33(Sup8):S10–s16. doi:10.12968/jowc.2023.0224
33. Murakami N, Asami Y, Yoshida H, et al. Distribution of genetic alterations in high-risk early-stage cervical cancer patients treated with postoperative radiation therapy. *Sci Rep*. 2021;11(1):10567. doi:10.1038/s41598-021-90139-0
34. Li X, Lu Y, Chen C, et al. Development and validation of a patient-specific model to predict postoperative SIRS in older patients: a two-center study. *Front Public Health*. 2023;11:1145013. doi:10.3389/fpubh.2023.1145013
35. Zhang L, Hu C, Li R, et al. The clinical predictive value of geriatric nutritional risk index in elderly rectal cancer patients received surgical treatment after neoadjuvant therapy. *Front Nutr*. 2023;10:1237047. doi:10.3389/fnut.2023.1237047
36. Ma G, Yan W, Yang Q, Li Y, Wang L. A nomogram and risk stratification for predicting subsyndromal delirium in elderly patients in a post-anaesthesia care unit: a prospective cohort study. *Int J Nurs Stud Adv*. 2025;9:100402. doi:10.1016/j.ijnsa.2025.100402
37. Imai H, Onozato R, Kaira K, et al. Course of postoperative relapse in non-small cell lung cancer is strongly associated with post-progression survival. *Thorac Cancer*. 2021;12(20):2740–2748. doi:10.1111/1759-7714.14119